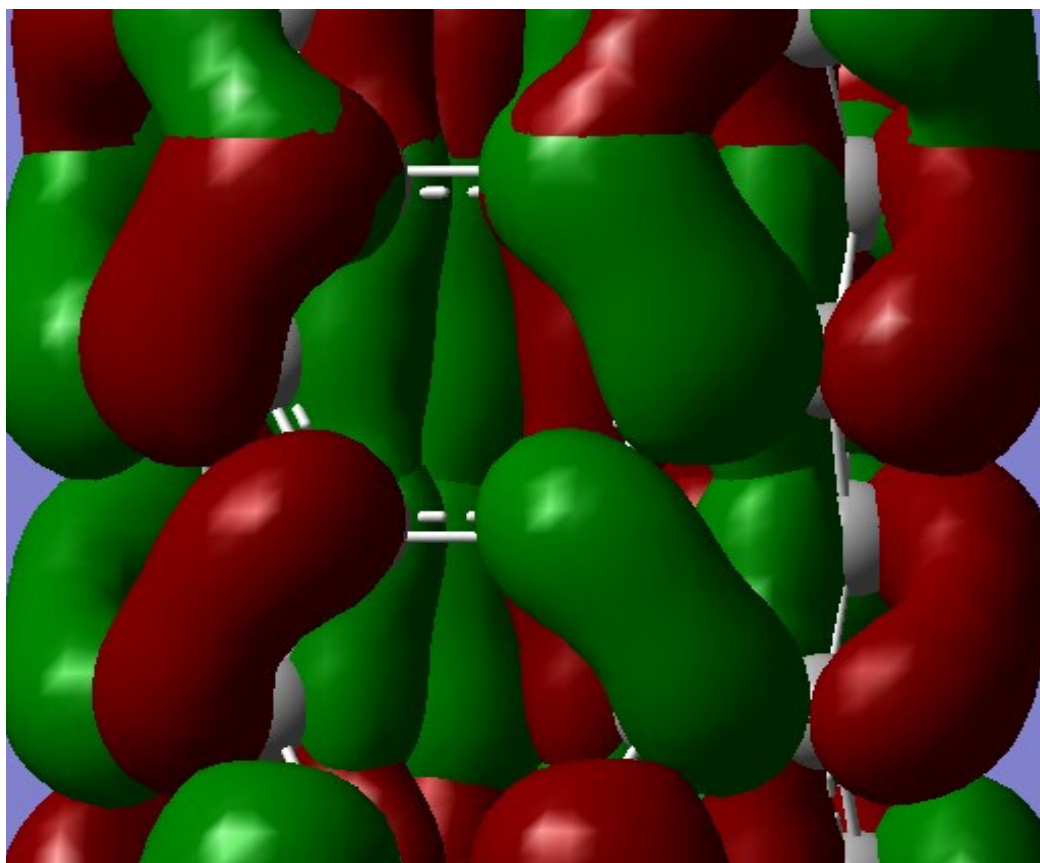


Volume 8, December 2019

ISSN 2542-2545

*The*  
**HIMALAYAN  
PHYSICS**

*A peer-reviewed Journal of Physics*



*Department of Physics, Prithvi Narayan Campus, Pokhara  
Nepal Physical Society, Western Chapter, Pokhara*

# A TB-LMTO approach to study structural stability and electronic behavior of transition metal dichalcogenides $\text{MX}_2$ (M=Zr, Hf AND X=S, Se)

Research Article

Saroj Kumar Chaudhary<sup>1</sup>, Gopi Chandra Kaphle<sup>1,2\*</sup>

1 Patan Multiple Campus, Tribhuvan University, Lalitpur, Nepal

2 Central Department of Physics, Tribhuvan University, Kirtipur, Nepal

3 Hydra Research and Policy Center, Kathmandu, Nepal

**Abstract:** We present a comprehensive first principles study on structural and electronic properties of TMDs  $\text{MX}_2$  (M=Zr, Hf AND X=S, Se) using Local Density Approximation (LDA) implemented Tight Binding Linear Muffin Tin Orbital (TB-LMTO) approach. The structural optimization of these materials are performed using energy minimization process. The optimized lattice parameters for  $\text{ZrS}_2$ ,  $\text{ZrSe}_2$ ,  $\text{HfS}_2$  and  $\text{HfSe}_2$  are found to be 3.71 Å, 3.70 Å, 3.62 Å, and 3.80 Å respectively. The band gaps of these materials are found to be 1.75 eV, 1.139 eV, 2.04 eV and 1.134 eV respectively which reveals the semi-conducting nature of  $\text{ZrS}_2$ ,  $\text{ZrSe}_2$  and  $\text{HfSe}_2$  while  $\text{HfS}_2$  is found to be insulator with large band gap. The density of states of these materials for up-spin and down-spin are found to be symmetric in nature showing non-magnetic behavior of these materials. The charge density plot of these materials along (100) plane and (110) plane shows covalent bond exist among (X-X) and (M-X) atoms while ionic bond exist among (M-M) atoms.

**Keywords:** Transition Metal Dichalcogenides • TBLMTO approach • Electronic properties • Band structure • Density of States

## 1. Introduction

Transition Metal Dichalcogenides TMDs  $\text{MX}_2$  where M is the transition metal and X is the chalcogen atom; are a class of compounds having both layered as well as non layered structure. Among 60 known TMDs, 40 TMDs assume layered type structure that have weak stacking of X-M-X sandwiches along hexagonal c-axis. TMDs have been a great sector for present research because of its diverse properties as well as applications in various fields of modern technology. After W. Fischer proposed the term “chalcogen” to denote the elements of group 16 in modern periodic table, those elements and their compounds have a great topic of research [1]. Since they exist in layered form along their hexagonal c-axis, they are used as great lubricants, and also suitable for capacitive devices. Doping of TMDs with other materials results in fascinating electronic properties so that they can be used as photonic devices due to the direct band gap, and are also suitable candidate for spintronic devices.

\* Corresponding Author: gck223@gmail.com

The first two-dimensional material known to the world; a one atom thick graphene was obtained in 2004 by scotch-tape method [2]. Due to its fantastic properties like ultrahigh mobility, superior mechanical strength etc. it has attracted the scientists all over the world. But due to the lack of energy band gap, it was difficult to use in logical electronic devices [3]. To overcome this difficulty, theoretical and experimental studies were done on bi-layer graphene [4, 5] but was found to be unsuccessful. So the research proceed towards other type of 2-D materials. Among them TMDs with favorable band gap attracted the attention of researchers. Since then, most of the works have been performed on single layered TMDs. TMDs with group VI(B) transition metals was extensively studied with great results [6, 7]. But only few works have been done on group IV(B) TMDs. Greenaway et. al. [8] performed an experimental study on optical properties of group IV-VI(B) chalcogenides with CdI<sub>2</sub> structure. Lee et. al. [9] performed experimental study on indirect band gap absorption edge of ZrS<sub>2</sub> and HfS<sub>2</sub>. Moustafa et. al. [10] also performed experimental study to know about growth and band gap determination of the Zr<sub>x</sub>Se<sub>2-x</sub> single crystal series. H. Jiang [11] studied the structural and electronic properties of ZrX<sub>2</sub> and HfX<sub>2</sub> using LDA and several variants of GGA and determined the structural properties, band structures, density of states etc. M. Abdulsalam [12] performed a detailed theoretical investigation on structural, electronic properties of different transition metal dichalcogenides using DFT, PAW based GGA and optical properties at GW and BSE level of approximation. Rasmussen et al. [13] performed first principle study on the electronic structure of 51 semi-conducting transition metal dichalcogenides in the G<sub>0</sub>W<sub>0</sub> approximation and compared the result with different density functional theory descriptions. Marias-Valero et al. [14] studied Raman spectra of ZrS<sub>2</sub> and ZrSe<sub>2</sub>. They reported the mechanical exfoliation of ZrX<sub>2</sub> (X=S, Se) from bulk to mono-layer. The result showed the possibility of obtaining atomically thin layers of ZrX<sub>2</sub> by mechanical exfoliation. Most of these works have been done on mono-layers TMDs and some works on 6 slab model [11] but few works on bulk structure have been done, so we are interested to study on bulk structure of these group IV(B) TMDs. Some papers show conflict result for the band gap of HfS<sub>2</sub>. [15] motivated us to go in detail through it. Similarly due to its potential use on various technological sectors such as Field-effect transistors, Photo-transistors, dielectric devices etc. [14, 15] attracted us towards the subject. Similarly one of the successful approach to study the electronic behavior and magnetic properties is Tight Binding Linear Muffin Tin Orbital within Atomic sphere approximation. A very few work have been performed previously on group IV(B) TMDs using this approximation [16, 16–18]. So we are greatly interested in applying this approach for the further investigation in the electronic properties of group IV(B) TMDs. Here, we have used four group IV(B) TMDs compounds ZrS<sub>2</sub>, ZrSe<sub>2</sub>, HfS<sub>2</sub> and HfSe<sub>2</sub> to know their properties in bulk state.

## 2. Computational Details

We have used first principles calculation to study the electronic structure of the TMDs material which includes the calculation of the ground state at first to find the minimized lattice parameter. Among the various

calculation methods used by our group [19–22], here we have used Local Density Approximation (LDA) implemented Tight Binding Linear Muffin Tin Orbital Atomic Sphere Approximation method [23]. The SCF solve the Kohn-Sham equation [24] using the exchange-correlation potential of Von Barth and Hedin with the help of minimal basis sets and partial wave method implemented in TB-LMTO-ASA code. In this approximation, the highly energetic valence electrons are included in the self consistent calculation process while deeper lying cores are treated as frozen state acts like ion called frozen core approximation. The linearized muffin-tin orbital method developed by Anderson uses a basis set for expanding the wave function, a set of orbitals that forms a complete basis set for a muffin-tin potential. The integration is performed in reciprocal space with 108 spatial k-points in the irreducible wedge of the Brillouin zone with default value of  $K_{cut}$  and  $E_{cut}$ . The default value of  $R_{MT}$  is used for individual atoms. Overall calculations were iterated to self consistency within the accuracy of  $10^{-6}$  Rydberg.

### 3. Results and Discussion

#### Structural analysis and lattice parameters

To investigate the electronic properties of group IV(B) TMDs, we have used the structural position and base parameters for  $MX_2$  from H. Jiang [11] with positions  $M = (0\ 0\ 0)$  and  $X = (1/3\ 2/3\ z)$  with  $CdI_2$  type IT structure resembling hexagonal symmetry. The space group number is 164 and P-3m1 in Hermann Mouglin notation. The Figs. 1(a) and 1(b) represent the optimized lattice parameter which is the plot of energy versus lattice parameter of  $ZrS_2$  and  $ZrSe_2$ . We found the most stable structure of  $ZrS_2$  and  $ZrSe_2$  is found when the lattice parameter is 3.63 Å and 3.70 Å which are found to be less than 5% deviated than the experimental value. The deviation in the parameters may be due to the calculating environment and experimental set up environment.

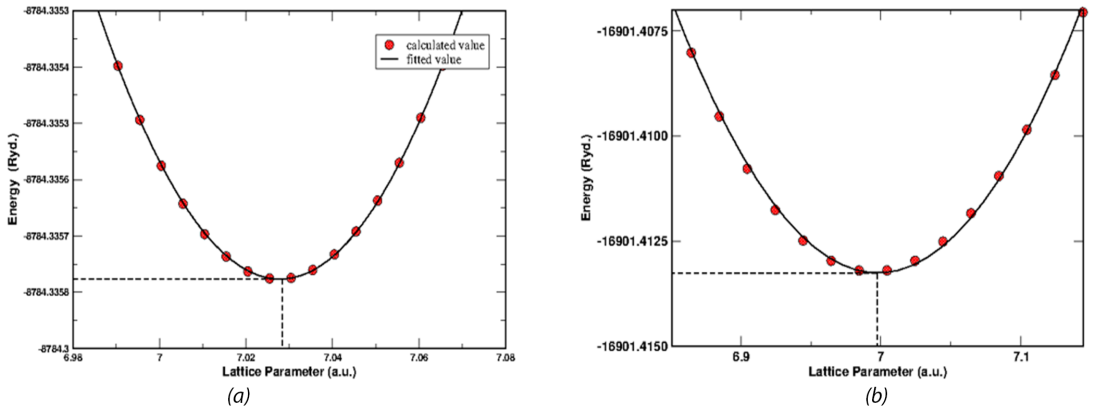


Figure 1. Plot of energy vs lattice parameter, (a)  $ZrS_2$ , and (b)  $ZrSe_2$ .

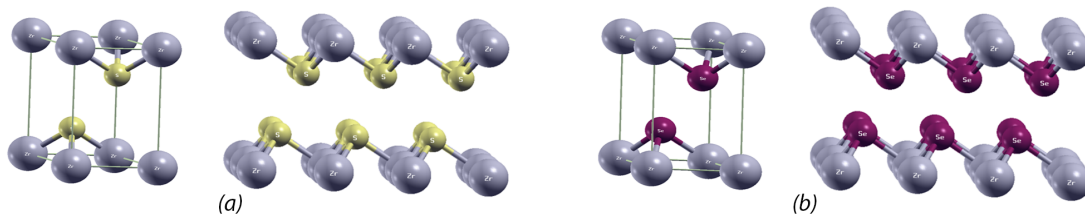


Figure 2. Primitive unit cell and  $3*2*1$  supershell showing layered structure, (a)  $ZrS_2$ , and (b)  $ZrSe_2$ .

Similarly the optimized lattice constant for  $HfS_2$  and  $HfSe_2$  are found to be  $3.62 \text{ \AA}$  and  $3.80 \text{ \AA}$  respectively. The calculated lattice parameter of  $HfS_2$  and  $HfSe_2$  are found to be less than 5% deviated from the experimental value. The energy minimization curve (Figs. 3(a-b)) along with primitive unit cell and supercell (Fig. 3(a-b)) are shown in figure below:

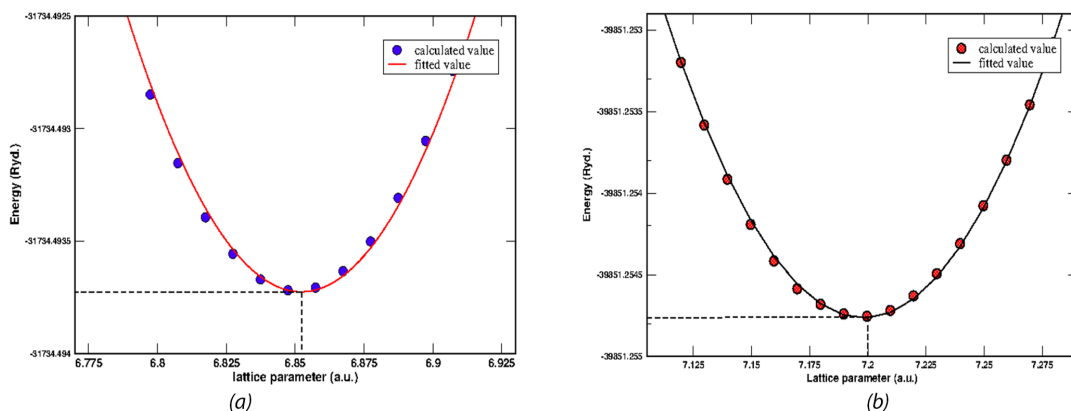


Figure 3. Plot of energy vs lattice parameter, (a)  $HfS_2$ , and (b)  $HfSe_2$ .

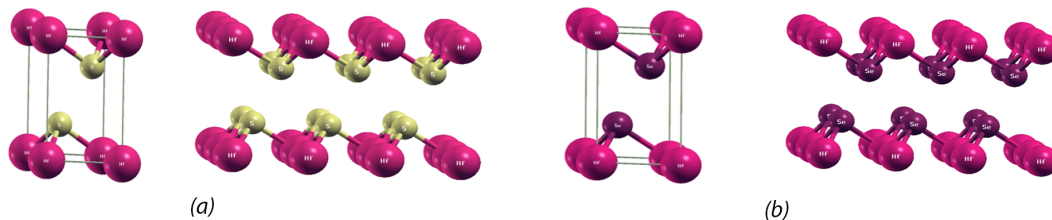


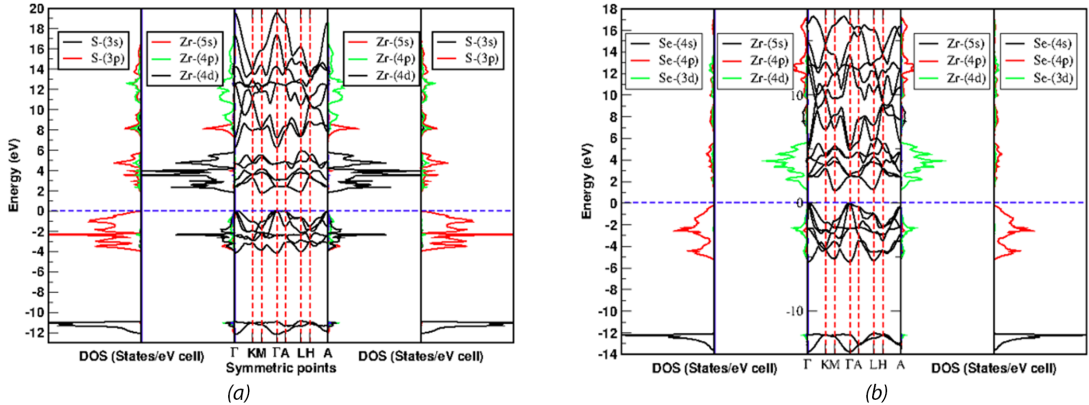
Figure 4. Primitive unit cell and  $3*2*1$  supershell showing layered structure, (a)  $HfS_2$ , and (b)  $HfSe_2$ .

Table 1. Lattice parameter and  $c/a$  ratio for group IVB TMDs  $MX_2$  ( $M=Zr, Hf$  and  $X=S, Se$ )

Properties	Bulk $ZrS_2$	Bulk $ZrSe_2$	Bulk $HfS_2$	Bulk $HfSe_2$
Lattice constant (a) ( $\text{\AA}$ )	3.71	3.70	3.62	3.80
$c/a$ ratio	1.573	1.608	1.598	1.637

## Electronic band structure and density of states analysis

Fig. 5(a) represents total band structure and its corresponding density of states. The first and fifth panel shows the up and down pdos of Sulfur while second and fourth panel shows up and down pdos of Zirconium in compound  $ZrS_2$ . The fifth panel shows the total band structure of  $ZrS_2$ . From the figure, we see that valence band maxima (VBM) lies at  $\Gamma$ -point whereas conduction band minima (CBM) lies at M-point. Since CBM and VBM lies at different points, the band is indirect in nature. Four major bands are seen. The first band lying between 6.21 eV to 19.44 eV show a mixture of 4p and 5s orbital of Zirconium and 3p orbital of Sulfur. Similarly the second band lying between 1.7 eV to 5.9 eV above the Fermi level indicates hybridization of 4d orbital of Zirconium and 3p orbital of Sulfur. The third band lying between -4.24 eV to 0 eV below the Fermi level is also a hybridization of 4d orbital of Zirconium and 3p orbital of Sulfur. The fourth band lying between -12.3 eV to -10.85 eV has a major contribution from 3s orbital of Sulfur. The symmetric nature of up and down spin channels reveals non magnetic behavior of  $ZrS_2$ .

Figure 5. Comparison of total band structure and partial density of states of different orbitals in  $ZrS_2$  and  $ZrSe_2$ 

Similarly the Fig. 5(b) is also a comparison of band structure and partial contribution to the density of states of Zirconium and Selenium in  $ZrSe_2$ . The structure is similar to compound  $ZrS_2$  in which valence band maximum lies at  $\Gamma$ -point. And conduction band minimum lies at M-point with a band gap of 1.139 eV. The band gap near Fermi level arises mainly due to the hybridization of 4d orbital of Zirconium and 4p orbital of Selenium.

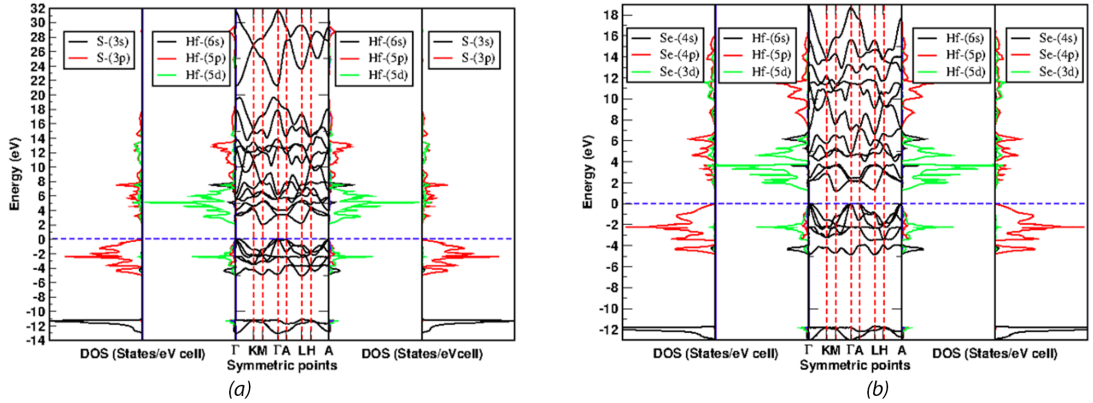


Figure 6. : Comparison of total band structure and partial density of states of different orbitals in  $\text{HfS}_2$  and  $\text{HfSe}_2$

Fig. 6(a) is the comparison of total band structure and partial density of states of different orbitals of  $\text{HfS}_2$ . From the above figure, it is seen that the band gap in  $\text{HfS}_2$  arises due to the hybridization of 4d orbital of Hafnium and 3p orbital of Sulfur near the Fermi level and the band gap is found to be 2.04 eV. Similarly, the Fig. 6(b) is also the comparison of total band structure and partial density of states of compound  $\text{HfSe}_2$ . The figure is similar to that of  $\text{HfS}_2$ . Here the band gap near Fermi level arises due to the hybridization of 5d orbital of Hafnium and 3d orbital of Selenium and the band gap is found to be 1.134 eV. Table 2 shows the comparison of band gap calculated by us and different experimental and theoretical results.

Table 2. Comparison of band gap from present calculations, previous calculations and Experimental value.

Materials (Bulk State)	Band gap (eV) (Present)	Band gap (eV) (experimental)	Band gap (eV) [11]
$\text{ZrS}_2$	1.75	1.7 [10]	0.79 (PBE)
		1.78 [25]	1.45(GW)
$\text{ZrSe}_2$	1.14	1.18 [10]	0.21 (PBE)
		1.20 [8]	0.89(GW)
$\text{HfS}_2$	2.04	1.96 [8]	0.90(PBE)
		2.13 [10]	1.80(GW)
$\text{HfSe}_2$	1.14	1.13 [8]	0.30(PBE)
		1.15 [26]	1.26(GW)

## Charge distribution analysis

The nature of the bond existing between the atoms present in a molecule can be analyzed with the help of charge density plot. Circular counters between the atoms show covalent nature of bond while non-circular and distorted counters shows a complex type of bond between the molecules. In covalent bond, large accumulation of charge is present between the atoms. The charge distribution at (100) and (110) planes of  $\text{HfSe}_2$  is as shown in

the Fig. 7.

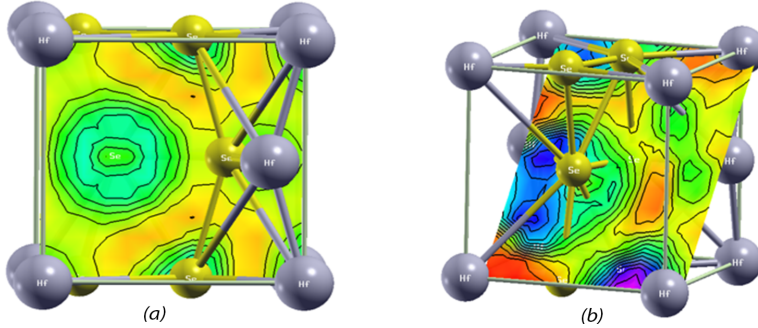


Figure 7. Charge distribution plot at, (a) (100), and (b) (110) plane in  $\text{HfSe}_2$

From the Fig. 7(a), we can see the symmetric and circular contours exist for Hf-Se (M-X) in (100) plane indicating covalent nature of bond between M and X. The overlapping and circular contours between Se-Se (X-X) atom in (110) plane in Fig. 7(b) indicates sharing of electron takes place which is basically covalent bond. Similarly contours in the plane (110) are non-symmetric and non-circular which shows charge transfer takes place between Hf-Hf (M-M) atom indicating ionic bond among X-M-X layer while weak Van der Waals bond lies between the layers.

## 4. Conclusions

We have performed structural and electronic analysis for four TMDs ( $\text{MX}_2$ ),  $\text{M}=\text{Zr}$ ,  $\text{Hf}$  and  $\text{X}=\text{S}$ ,  $\text{Se}$ . At first structural optimization through energy minimization process is performed to calculate the lattice parameters. The lattice parameters of  $\text{ZrS}_2$ ,  $\text{ZrSe}_2$ ,  $\text{HfS}_2$  and  $\text{HfSe}_2$  are found to be 3.71 Å, 3.70 Å, 3.62 Å, and 3.80 Å respectively which are less than 3% deviated than the experimental values. The band structure is calculated through LDA +U approach within TB-LMTO-ASA approximation. The band gap of  $\text{ZrS}_2$ ,  $\text{ZrSe}_2$ ,  $\text{HfS}_2$  and  $\text{HfSe}_2$  are found to be 1.75 eV, 1.139 eV, 2.04 eV and 1.134 eV respectively which reveals the semi conducting nature of  $\text{ZrS}_2$ ,  $\text{ZrSe}_2$  and  $\text{HfSe}_2$  while  $\text{HfS}_2$  is found to be insulator with large band gap. The band gap in  $\text{ZrS}_2$  and  $\text{ZrSe}_2$  arises mainly due to the hybridization 4d orbital of Zirconium and 3p orbital of Sulfur and 4p orbital of Selenium. Similarly in  $\text{HfS}_2$  and  $\text{HfSe}_2$  the band gap arises due to the hybridization of 5d orbital of Hafnium and 3p orbital of Sulfur and 4p orbital of Selenium. The density of state analysis supports the result. The charge density plot shows that covalent bond exist between non-metal atoms (X-X) and between metal and non-metal atoms (M-X) while ionic bond exist between the metal (M-M) atoms among X-M-X layer while weak Van der Waals bond exist between the layers.

## 5. Acknowledgements

Hydra Research and Policy Centre (HRPC) Nepal is acknowledged for partial support. A Mookerjee of SNBNCBS, Kolkota and N. P. Adhikari of CDP, TU are acknowledged for the computational code and discussion during the preparation of manuscript.

### References

- 
- [1] Fischer W. A second note on the term "chalcogen". *Journal of Chemical Education*. 2001;78(10):1333.
  - [2] Novoselov KS, Geim A. The rise of graphene. *Nat Mater*. 2007;6(3):183–191.
  - [3] Neto AC, Guinea F, Peres NM, Novoselov KS, Geim AK. The electronic properties of graphene. *Reviews of modern physics*. 2009;81(1):109.
  - [4] Ohta T, Bostwick A, Seyller T, Horn K, Rotenberg E. Controlling the electronic structure of bilayer graphene. *Science*. 2006;313(5789):951–954.
  - [5] Zhang Y, Tang TT, Girit C, Hao Z, Martin MC, Zettl A, et al. Direct observation of a widely tunable bandgap in bilayer graphene. *Nature*. 2009;459(7248):820–823.
  - [6] Novoselov KS, Jiang D, Schedin F, Booth T, Khotkevich V, Morozov S, et al. Two-dimensional atomic crystals. *Proceedings of the National Academy of Sciences*. 2005;102(30):10451–10453.
  - [7] Yan Q, Huang B, Yu J, Zheng F, Zang J, Wu J, et al. Intrinsic current-voltage characteristics of graphene nanoribbon transistors and effect of edge doping. *Nano letters*. 2007;7(6):1469–1473.
  - [8] Greenaway DL, Nitsche R. Preparation and optical properties of group IV–VI<sub>2</sub> chalcogenides having the CdI<sub>2</sub> structure. *Journal of Physics and Chemistry of Solids*. 1965;26(9):1445–1458.
  - [9] Lee P, Said G, Davis R, Lim T. On the optical properties of some layer compounds. *Journal of Physics and Chemistry of Solids*. 1969;30(12):2719–2729.
  - [10] Moustafa M, Zandt T, Janowitz C, Manzke R. Growth and band gap determination of the ZrS<sub>x</sub>Se<sub>2-x</sub> single crystal series. *Physical Review B*. 2009;80(3):035206.
  - [11] Jiang H. Structural and electronic properties of ZrX<sub>2</sub> and HfX<sub>2</sub> (X= S and Se) from first principles calculations. *The Journal of chemical physics*. 2011;134(20):204705.
  - [12] Abdulsalam M, Moise D, Joubert DP. Electronic and Optical Properties of monolayer MX<sub>2</sub> (M= Zr, Hf; X= S, Se) from first principles calculations;.
  - [13] Rasmussen FA, Thygesen KS. Computational 2D materials database: electronic structure of transition-metal dichalcogenides and oxides. *The Journal of Physical Chemistry C*. 2015;119(23):13169–13183.
  - [14] Mañas-Valero S, García-López V, Cantarero A, Galbiati M. Raman spectra of ZrS<sub>2</sub> and ZrSe<sub>2</sub> from bulk to atomically thin layers. *Applied sciences*. 2016;6(9):264.
  - [15] Traving M, Seydel T, Kipp L, Skibowski M, Starrost F, Krasovskii E, et al. Combined photoemission and

- inverse photoemission study of HfS 2. *Physical Review B*. 2001;63(3):035107.
- [16] Pandey S, Kaphle GC, Adhikari NP. Electronic structure and magnetic properties of bulk elements (Fe and Pd) and ordered binary alloys (FePd and Fe<sub>3</sub>Pd): TB-LMTO-ASA. *BIBECHANA*. 2014;11:60–69.
- [17] Sharma P, Kaphle GC. Electronic and Magnetic Properties of Half Metallic Heusler Alloy Co<sub>2</sub>MnSi: A First-Principles Study. *Himalayan Physics*. 2017;p. 31–36.
- [18] Sedhain RP, Kaphle GC. Structural and Electronic Properties of Transition Metal Di-chalcogenides (MX<sub>2</sub>) M=(Mo, W) and X=(S, Se) in Bulk State: a First-principles Study. *Journal of Institute of Science and Technology*. 2017;22(1):41–50.
- [19] Kaphle GC, Ganguly S, Banerjee R, Banerjee R, Khanal R, Adhikari CM, et al. A study of magnetism in disordered Pt–Mn, Pd–Mn and Ni–Mn alloys: an augmented space recursion approach. *Journal of Physics: Condensed Matter*. 2012;24(29):295501.
- [20] Kaphle GC, Adhikari N, Mookerjee A. Study of Spin Glass Behavior in Disordered Pt x Mn<sub>1-x</sub> Alloys: An Augmented Space Recursion Approach. *Advanced Science Letters*. 2015;21(9):2681–2687.
- [21] Datta S, Kaphle GC, Baral S, Mookerjee A. Study of morphology effects on magnetic interactions and band gap variations for 3 d late transition metal bi-doped ZnO nanostructures by hybrid DFT calculations. *The Journal of chemical physics*. 2015;143(8):084309.
- [22] Adhikari PR, Upadhyay OP, Kaphle GC, Srivastava A. Electronic and structural study of hexagonal TiC nanowires: ab initio study. *BIBECHANA*. 2019;16:7–14.
- [23] Anisimov VI, Aryasetiawan F, Lichtenstein A. First-principles calculations of the electronic structure and spectra of strongly correlated systems: the LDA+ U method. *Journal of Physics: Condensed Matter*. 1997;9(4):767.
- [24] Kohn W, Sham LJ. Self-consistent equations including exchange and correlation effects. *Physical review*. 1965;140(4A):A1133.
- [25] Roubi L, Carlone C. Resonance raman spectrum of HfS 2 and ZrS 2. *Physical Review B*. 1988;37(12):6808.
- [26] Gaiser C, Zandt T, Krapf A, Serverin R, Janowitz C, Manzke R. Band-gap engineering with HfS x Se 2- x. *Physical Review B*. 2004;69(7):075205.